Inorganic Chemistry
Article

Inorg. Chem. **2010**, *49*, 2407–2415 **2407**
DOI: 10.1021/ic902257u

Synthesis, Crystal Structure, and Photoluminescence of Homodinuclear Lanthanide 4-(Dibenzylamino)benzoate Complexes

A. R. Ramya,[†] M. L. P. Reddy,*[,†] Alan H. Cowley,[‡] and Kalyan V. Vasudevan[‡]

[†]*Chemical Sciences and Technology Division, National Institute for Interdisciplinary Science & Technology (NIIST), CSIR, Thiruvananthapuram-695 019, India, and* [‡]*Department of Chemistry and Biochemistry, The University of Texas at Austin, 1 University Station A5300, Austin, Texas 78712*

Received November 15, 2009

Three new binuclear lanthanide complexes of general formula $[Ln_2(L)_6(H_2O)_4]$ (Ln = Tb (**1**), Eu (**2**), and Gd (**3**)) supported by the novel aromatic carboxylate ligand 4-(dibenzylamino)benzoic acid (HL) have been synthesized. Complexes **1** and **2** were structurally characterized by single-crystal X-ray diffraction. Both **1** and **2** crystallize in the triclinic space group $P\bar{1}$, and their molecular structures consist of homodinuclear species that are bridged by two oxygen atoms from two carboxylate ligands via different coordination modes. The discrete bridged dimer of **1** is centrosymmetric and features 8-coordinate terbium atoms, each of which adopts a distorted square-antiprismatic geometry. Both coordination spheres comprise two η^2-chelating benzoates, two μ-η^1:η^1-carboxylate interactions from the bridging benzoates, and two water molecules. By contrast, in complex **2**, the Eu^{3+} ion coordination environment is best described as a distorted tricapped-trigonal prism, each europium ion being coordinated to three η^2-chelating benzoate ligands and two water molecules. One of the η^2-carboxylate ligands is involved in a further interaction with an adjacent metal, thus rendering the overall binding mode bridging tridentate, μ-η^2:η^1. Scrutiny of the packing diagrams for **1** and **2** revealed the existence of a one-dimensional molecular array that is held together by intermolecular hydrogen-bonding interactions. The Tb^{3+} complex **1** exhibits high green luminescence efficiency in the solid state with a quantum yield of 82%. On the other hand, poor luminescence efficiency has been noted for the Eu^{3+}−4-(dibenzylamino)benzoate complex.

Introduction

The unique electronic structures of lanthanide cations ligated with conjugated organic ligands continue to stimulate an ever increasing number of important technological applications in fields as diverse as biomedicine and materials science.[1−5] Moreover, the long excited-state lifetimes and the high chromaticities of the lanthanides are also pertinent to applications in the domain of solid-state photonic materials. For instance, Tb^{3+}, Eu^{3+}, and Tm^{3+} cations are used as green, red, and blue emitters, respectively, in multicolor displays and organic light-emitting diodes (OLEDs).[6] However, since f−f transitions are parity forbidden, unligated luminescent lanthanide cations have extremely low molar extinction coefficients; hence, direct lanthanide excitation results only in modest luminescence intensities.[7] Therefore, over the past few years, efforts have been made to augment the absorption coefficients and thereby obtain significantly more intense lanthanide ion emissions. Fortunately, this objective can be accomplished by prudent selection and synthesis of organic ligands with conjugated motifs. Aromatic carboxylic acids[8] and β-diketones[9] are particularly

*To whom correspondence should be addressed. E-mail: mlpreddy55@gmail.com.

(1) (a) Bünzli, J.-C. G.; Piguet, C. *Chem. Soc. Rev.* **2005**, *34*, 1048–1077. (b) Bünzli, J.-C. G. *Acc. Chem. Res.* **2006**, *39*, 53–61. (c) de Bettencourt-Dias, A. *Dalton Trans.* **2007**, *22*, 2229–2241. (d) Kuriki, K.; Koike, Y.; Okamoto, Y. *Chem. Rev.* **2002**, *102*, 2347–2356.

(2) (a) Binnemans, K. *Chem. Rev.* **2009**, *109*, 4283–4374. (b) Moore, E. G.; Samuel, A. P. S.; Raymond, K. N. *Acc. Chem. Res.* **2009**, *42*, 542–552.

(3) (a) A. Picot, A.; Aleo, A. D.; Baldeck, P. L.; Grichine, A.; Duperray, A.; Andraud, C.; Maury, O. *J. Am. Chem. Soc.* **2008**, *130*, 1532–1533. (b) Parker, D.; Williams, J. A. G. *The Lanthanides and Their Interrelation with Biosystems*; M. Dekker, Inc.: New York, 2003; Vol. *40*, p 2337. (c) Parker, D. *Chem. Soc. Rev.* **2004**, *33*, 156–165.

(4) (a) Pandya, S.; Yu, J.; Parker, D. *Dalton Trans.* **2006**, *23*, 2757–2766. (b) Gunnlaugsson, D .; Leonard, J. P. *Chem. Commun.* **2005**, *25*, 3114–3131.

(5) Brunet, E.; Juanes, O.; Rodriguez-Ubis, J. C. *Curr. Chem. Biol.* **2007**, *1*, 11–39.

(6) (a) Jüstel, T.; Nikol, H.; Ronda, C. *Angew. Chem., Int. Ed.* **1998**, *37*, 3084–3103. (b) Hao, J.; Studenikin, S. A.; Cocivera, M. *J. Lumin.* **2001**, *93*, 313–319.

(7) (a) Carnall, W. T.; Gruen, D. M.; McBeth, R. L. *J. Phys. Chem.* **1962**, *66*, 2159. (b) Carnall, W. T. *J. Phys. Chem.* **1963**, *67*, 1206. (c) Carnall, W. T.; Fields, P. R.; Wybourne, B. G. *J. Chem. Phys.* **1965**, *42*, 3797. (d) Kim, Y. H.; Baek, N. S.; Kim, H. K. *Chem. Phys. Chem.* **2006**, *7*, 213–221.

(8) (a) Eddaudi, M.; Kim, J.; Wachter, J. B.; Chae, H. K.; O'Keeffe, M.; Yaghi, O. M. *J. Am. Chem. Soc.* **2001**, *123*, 4368–4369. (b) Pan, L.; Sander, M. B.; Huang, X.; Li, J.; Smith, M.; Bittner, E.; Bockrath, B.; Johnson, J. K. *J. Am. Chem. Soc.* **2004**, *126*, 1308–1309. (c) Chen, X. Y.; Bretonniere, Y.; Pecaut, J.; Imbert, D.; Bünzli, J. -C. G.; Mazzanti, M. *Inorg. Chem.* **2007**, *46*, 625–637. (d) Zhou, X.-X.; Cai, Y.-P.; Zhu, S.-Z.; Zhan, Q.-G.; Liu, M.-S.; Zhou, Z.-Y.; Chen, L. *Cryst. Growth Des.* **2008**, *8*, 2076–2079. (e) Louise, S.; Natrajan, L. S.; Phillipa, L.; Timmins, P. L.; Matthew Lunn, M.; Heath, S. L. *Inorg. Chem.* **2007**, *46*, 10877–10886.

Published on Web 02/02/2010

valuable in this context because such ligands can absorb ultraviolet light and transfer the absorbed energy to the central lanthanide ions in an appropriately effective manner (the so-called antenna effect).[10] In particular, when aromatic carboxylic acids are employed as the antenna ligands, the coordinated lanthanide ions exhibit higher luminescent stabilities than those ligated with other organic ligands.[11] This enhanced stability is of obvious practical importance in terms of device performance and stability.

A number of lanthanide benzoate coordination complexes with unique photophysical properties[12] and intriguing structural features[13] have been disclosed recently. The benzoate ligands were selected on the basis of the fact that carboxylate groups interact strongly with the oxophilic lanthanoids and the fact that the delocalized π-electron system provides a strongly absorbing chromophore.[12,14] Prior results suggested that derivitization of the benzoic acid analogues with thiophene had a beneficial effect in terms of tuning the triplet state of the antenna. In particular, the enhanced emission quantum yield originated from a better match between the pertinent ligand orbitals and lanthanide ion excited states.[15] The intense fluorescent emissions of homodinuclear lanthanide complexes of 4-cyanobenzoic acid imply that the ligand-to-Ln^{3+} energy transfer is efficient and that coordinated water molecules do not quench the luminescence by nonradiative dissipation of energy.[16] Very high quantum yields (88%) have been reported with terbium−aminobenzoate complexes,[17] which is somewhat surprising in view of the coordination of both $-NH_2$ and OH_2 ligands, since such moieties usually function as vibrational deactivators of the excited state.[18]

Given the important potential applications of lanthanide carboxylates and the fascinating properties of benzoate ligands, we were prompted to prepare a new series of lanthanide complexes featuring the 4-(dibenzylamino)benzoic acid ligand by replacing the hydrogens of the $-NH_2$ group with benzyl groups. The highly conjugated benzoic acid functionality has a significant influence on the distribution of π-electron density within the ligand system. Accordingly, the effective charges on the atoms coordinated to the Ln^{3+} ions can be changed, and the interaction of the ligand with metal ion can be modified. As a consequence, the energies of the ligand−metal charge transfer states (LMCTs) and the position of the triplet level are changed, which in turn has profound effects on the luminescent properties of various Ln^{3+} ions. In the present work, a new derivative of benzoic acid has been designed, characterized, and utilized for the synthesis of the desired Tb^{3+}, Eu^{3+}, and Gd^{3+} complexes. Two of the new lanthanide 4-(dibenzylamino)benzoates have been structurally characterized by single-crystal X-ray diffraction, and the photophysical properties of all three of the new lanthanide benzoate complexes have been investigated and correlated with the triplet energy levels of the designed ligand.

Experimental Section

Materials and Instrumentation. The following chemicals were procured commercially and used without further purification: terbium(III) nitrate hexahydrate, 99.9% (Acros Organics); europium(III) nitrate hexahydrate, 99.9% (Acros Organics); gadolinium(III) nitrate hexahydrate (Treibacher); methyl 4-aminobenzoate, 98% (Aldrich); and benzyl bromide, 99.9% (Aldrich). All of the other chemicals used were of analytical reagent grade.

Elemental analyses were performed with a Perkin-Elmer Series 2 Elemental Analyzer 2400. A Perkin-Elmer Spectrum One FT-IR spectrometer was used to obtain the IR spectral data (neat KBr), and a Bruker 500 MHz NMR spectrometer was used to record the ^1H NMR and ^{13}C NMR (125 MHz) spectra of the ligands in $CDCl_3$ solution. The mass spectra were recorded on a JEOL JSM 600 fast atom bombardment (FAB) high resolution mass spectrometer (FABMS), and the thermogravimetric analyses were performed on a TG/DTA-6200 (SII Nano Technology Inc., Japan). The absorbances of the ligands were measured in $CHCl_3$ solution on a UV−vis spectrophotometer (Shimadzu, UV-2450), and the photoluminescence (PL) spectra were recorded on a Spex-Fluorolog FL22 spectrofluorimeter equipped with a double grating 0.22 m Spex 1680 monochromator and a 450W Xe lamp as the excitation source operating in the front face mode. The lifetime measurements were carried out at room temperature using a Spex 1040D phosphorimeter.

The overall quantum yields ($\Phi_{overall}$) were measured using an integrating sphere in a SPEX Fluorolog spectrofluorimeter. The PL quantum yields of thin films ($\Phi_{overall}$) were determined using a calibrated integrating sphere system. A Xe-arc lamp was used to excite the thin film samples that were placed in the sphere. All samples were prepared by drop casting the material placed between two quartz coverslips. The quantum yields were determined by comparing the spectral intensities of the lamp and the sample emission as reported in the literature.[19] Using this experimental setup and the integrating sphere system, the solid state fluorescence quantum yield of a thin film of the standard green OLED material tris-8-hydroxyquinolinolato aluminum (Alq_3) was determined to be 0.19, which is consistent with previously reported values.[20] Each sample was measured several

(9) (a) de Sa, G. F.; Malta, O. L.; de Mello Donega, C.; Simas, A. M.; Longo, R. L.; Santa-Cruz, P. A.; da Silva, E. F., Jr. *Coord. Chem. Rev.* **2000**, *196*, 165–195. (b) Binnemans, K.; Gorller-Walrand, C. *Chem. Rev.* **2002**, *102*, 2303–2345. (c) Biju, S.; Ambili Raj, D. B.; Reddy, M. L. P.; Kariuki, B. M. *Inorg. Chem.* **2006**, *45*, 10651–10660. (d) Zheng, Y.; Cardinali, F.; Armaroli, N.; Accorsi, G. *Eur. J. Inorg. Chem.* **2008**, *28*, 2075–2080. (e) Fratini, A.; Richards, G.; Larder, E.; Swavey, S. *Inorg. Chem.* **2008**, *47*, 1030–1036.

(10) (a) Lehn, J. M. *Angew. Chem., Int. Ed.* **1990**, *29*, 1304–1319. (b) Kido, J.; Okamoto, Y. *Chem. Rev.* **2002**, *102*, 2357–2368. (c) Bünzli, J.-C. G.; Piguet, C. *Chem. Rev.* **2002**, *102*, 1897–1928. (d) Parker, D. *Coord. Chem. Rev.* **2000**, *205*, 109–130. (e) Piguet, C.; Bünzli, J.-C. G. *Chem. Soc. Rev.* **1999**, *28*, 347–358. (f) Petoud, S.; Cohen, S. M.; Bünzli, J.-C. G.; Raymond, K. N. *J. Am. Chem. Soc.* **2003**, *125*, 13324–13325.

(11) (a) Shyni, R.; Biju, S.; Reddy, M. L. P.; Cowley, A. H.; Findlater, M. *Inorg. Chem.* **2007**, *46*, 11025–11030. (b) Raphael, S.; Reddy, M. L. P.; Cowley, A. H.; Findlater, M. *Eur. J. Inorg. Chem.* **2008**, *28*, 4387–4394.

(12) (a) Hilder, M.; Junk, P. C.; Kynast, U. H.; Lezhnina, M. M. *J. Photochem. Photobiol. A: Chem.* **2009**, *202*, 10–20. (b) Tsaryuk, V.; Zhuravlev, K.; Zolin, V.; Gawryszewska, P.; Legendziewicz, P.; Kudryashova, V.; Pekareva, I. *J. Photochem. Photobiol. A: Chem.* **2006**, *177*, 314–323.

(13) (a) Busskamp, H.; Deacon, G. B.; Hilder, M.; Junk, P. C.; Kynast, U. H.; Lee, W. W.; Turner, D. R. *Cryst. Eng. Comm.* **2007**, *9*, 394–411. (b) Deacon, G. B.; Hein, S.; Junk, P. C.; Justel, T.; Lee, W.; Turner, D. R. *Cryst. Eng. Comm.* **2007**, *9*, 1110–1123. (c) Zhong, R.; Zou, R.; Du, M.; Jiang, L.; Yamada, T.; Maruta, G.; Takeda, S.; Xu, Q. *Cryst. Eng. Comm.* **2008**, *10*, 605–613.

(14) de Bettencourt-Dias, A.; Viswanathan, S. *Dalton Trans.* **2006**, *34*, 4093–4103.

(15) Viswanathan, S.; de Bettencourt-Dias, A. *Inorg. Chem.* **2006**, *45*, 10138–10146.

(16) Li, Y.; Zheng, F. K.; Liu, X.; Zou, W. Q.; Guo, G. C.; Lu, C. Z.; Huang, J. S. *Inorg. Chem.* **2006**, *45*, 6308–6316.

(17) Fiedler, T.; Hilder, M.; Junk, P. C.; Kynast, U. H.; Lezhnina, M. M.; Warzala, M. *Eur. J. Inorg. Chem.* **2007**, *2*, 291–301.

(18) Sabbatini, N.; Guardigli, M.; Lehn, J. M. *Coord. Chem. Rev.* **1993**, *123*, 201–228.

(19) (a) De Mello, C.; Wittmann, H. F.; Friend, R. H. *Adv. Mater.* **1997**, *9*, 230–232. (b) Pålsson, L.-O.; Monkman, A. P. *Adv. Mater.* **2002**, *14*, 757–758. (c) Shah, B. K.; Neckers, D. C.; Shi, J.; Forsythe, E. W.; Morton, D. *Chem. Mater.* **2006**, *18*, 603–608.

(20) (a) Colle, M.; Gmeiner, J.; Milius, W.; Hillebrecht, H.; Brütting, W. *Adv. Funct. Mater.* **2003**, *13*, 108–112. (b) Saleesh Kumar, N. S.; Varghese, S.; Rath, N. P.; Das, S. *J. Phys. Chem. C* **2008**, *112*, 8429–8437.

times under slightly different experimental conditions. The estimated error for the quantum yields is ±10%.[21] For measuring the quantum yield by the relative method, the diffuse reflectance spectra of the new lanthanide complexes and the standard phosphor were recorded on a Shimadzu UV-2450 UV−vis spectrophotometer using $BaSO_4$ as a reference. The overall quantum yields ($\Phi_{overall}$), were measured at room temperature using the technique for powdered samples described by Bril and De Jager-Veenis,[22] along with the following expression:

$$\phi_{overall} = \frac{1-r_{st}}{1-r_x} \times \frac{A_x}{A_{st}} \times \phi_{st} \quad (1)$$

where r_x and r_{st} represent the diffuse reflectance of the complexes and the standard phosphor, respectively (with respect to a fixed wavelength), and Φ_{st} is the quantum yield of the standard phosphor. The terms A_x and A_{st} represent the areas under the complex and the standard emission spectra, respectively. To acquire absolute intensity values, $BaSO_4$ was used as a reflecting standard. The standard phosphor used was pyrene (Aldrich), the emission spectrum of which comprises a large broad band peaking around 471 nm, with a constant Φ value (Φ_{st} = 61%, λ_{ex} = 313 nm).[23] Three measurements were carried out for each sample, and the reported $\Phi_{overall}$ value corresponds to the arithmetic mean value of the three values. The errors in the quantum yield values associated with this technique were estimated to be within ±10%.[24]

The X-ray diffraction data were collected at 153 K on a Nonius Kappa CCD diffractometer equipped with an Oxford Cryostream low-temperature device and a graphite-monochromated Mo Kα radiation source (λ = 0.71073 Å). Corrections were applied for Lorentz and polarization effects.[25] Both structures were solved by direct methods and refined by full-matrix least-squares cycles on F^2. All of the nonhydrogen atoms were allowed anisotropic thermal motion, and the hydrogen atoms were placed in fixed, calculated positions using a riding model (C−H, 0.96 Å). Selected crystal data and data collection and refinement parameters are listed in Table 1. X-ray crystallographic information files can be obtained free of charge via www.ccdc.cam.ac.uk/consts/retrieving.html (or from CCDC, 12 Union Road, Cambridge CB2 1EZ, U.K.; fax, +44 1223 336033; e-mail, deposit@ccdc.cam.ac.uk). The CCDC numbers are 743231 and 746200 for **1** and **2**, respectively. A molecule of DMSO has been added to the molecular formulas of **1** and **2** since in each case it was removed via "Squeeze" due to the extreme disorder which could not be solved. Furthermore, the water protons were not located, and the hydroxyl protons have been placed in the positions that were calculated on the basis of optimum hydrogen bonding.

Synthesis of Methyl 4-(Dibenzylamino)benzoate. Potassium carbonate (0.68 g, 4.92 mmol) was added to a solution of methyl 4-amino benzoate (0.25 g, 1.65 mmol) in freshly distilled DMF (50 mL). The resulting reaction mixture was refluxed for 30 min, following which benzyl bromide (0.56 g, 3.29 mmol) was added, and the solution was refluxed at 78 °C for an additional 48 h. The reaction mixture was then poured into water, and the resulting precipitate was filtered off, washed with water, and dried. The resulting residue was purified by silica gel column chromatography using hexane/ethyl acetate, thereby affording the desired product as a white solid. Yield, 0.2 g (36.4%). ^{1}H NMR (500 MHz, $CDCl_3$): δ (ppm) 7.85 (d, 2H, J = 9 Hz, Ar−H), 7.34 (t, 4H, J = 7 Hz, Ar−H), 7.27 (t, 2H, J = 7.5 Hz, Ar−H), 7.21 (d, 4H, J = 7 Hz, Ar−H), 6.72 (d, 2H, J = 9 Hz, Ar−H), 4.71 (S, 4H, $-NCH_2$), 3.83 (S, 3H, $-OCH_3$). ^{13}C NMR (125 MHz, $CDCl_3$): δ (ppm) 167.26, 152.54, 137.37, 131.48, 128.83, 127.24, 126.45, 117.93, 111.26, 53.98, 51.53. MS (FAB) m/z = 332.53 $(M + 1)^+$. FT-IR (KBr) ν_{max}: 1690 (ν_{as}(C═O)), 1432 (ν_s(C═O)), 1600, 1530, 1313, 1280, 1174, 1113, 834, 768 cm^{-1}.

Table 1. Crystallographic and Refinement Data for **1** and **2**

	1	**2**
formula	$C_{130}H_{136}N_6O_{22}S_2Tb_2$	$C_{130}H_{128}N_6O_{18}S_2Eu_2$
fw	2516.41	2430.42
cryst syst	triclinic	triclinic
space group	$P\bar{1}$	$P\bar{1}$
cryst size	0.25 × 0.22 × 0.15	0.24 × 0.20 × 0.13
temp/K	153(2)	153(2)
a (Å)	9.829(5)	9.879(5)
b (Å)	17.180(5)	17.259(5)
c (Å)	17.816 (5)	17.896 (5)
α (deg)	84.917 (5)	85.264(5)
β (deg)	82.794 (5)	83.206 (5)
γ (deg)	87.271(5)	88.609 (5)
V/Å^3	2971.2 (19)	3019(2)
Z	1	1
D_{calcd}, g cm^{-1}	1.406	1.337
μ(Mo,Kα), mm^{-1}	1.288	1.131
F(000)	1296	1252
R1 [$I > 2\sigma(I)$]	0.0396	0.0521
wR2 [$I > 2\sigma(I)$]	0.0872	0.1146
R1 (all data)	0.0532	0.0996
wR2 (all data)	0.0915	0.1246
GOF	1.093	1.023

Synthesis of 4-(Dibenzylamino)benzoic Acid (HL). Methyl 4-(dibenzylamino)benzoate (0.3 g, 0.902 mmol) was refluxed for 24 h in a solution of KOH (0.15 g, 2.67 mmol) in 50 mL of ethanol. The reaction mixture was poured into ice cold water and acidified with dilute HCl, and the resulting precipitate was filtered, washed, dried, and recrystallized from CH_2Cl_2. Yield, 0.25 g (87%): ^{1}H NMR (500 MHz, $CDCl_3$): δ (ppm) 7.92 (d, 2H, J = 9.5 Hz, Ar−H), 7.36 (t, 4H, J = 7 Hz, Ar−H), 7.29 (t, 2H, J = 7 Hz, Ar−H), 7.23 (d, 4H, J = 7 Hz, Ar−H), 6.74 (d, 2H, J = 9 Hz, Ar−H), 4.74 (s, 4H, $-NCH_2$). ^{13}C NMR (125 MHz, $CDCl_3$): δ (ppm) 172.06, 153.17, 137.21, 132.26, 128.87, 127.29, 126.43, 116.92, 111.27, 53.99. MS (FAB) m/z = 318.57 $(M + 1)^+$. Elemental analysis (%) calcd (found) for $C_{21}H_{19}O_2N$ (317.381): C, 79.47 (79.00); H, 6.03 (6.27); N, 4.41 (4.36). FT-IR (KBr), ν_{max}: 1663 (ν_{as}(C═O)), 1450 (ν_s(C═O)), 1599, 1557, 1529, 1450, 1413, 1363, 1288, 723, 694 cm^{-1}.

Syntheses of Lanthanide Complexes. In a typical procedure, an ethanolic solution of $Ln(NO_3)_3 \cdot 6H_2O$ (0.5 mmol) (Ln = Eu, Tb, or Gd) was added to a solution of 4-(dibenzylamino)benzoic acid (1.5 mmol) in ethanol in the presence of NaOH (1.5 mmol). Precipitation took place immediately, and the reaction mixture was stirred subsequently for 10 h at room temperature. The crude product was filtered, washed with ethanol, and dried. The resulting complexes were then purified by recrystallization from a dichloromethane/methanol solvent mixture. Single crystals of the terbium and europium complexes suitable for X-ray study were obtained from a dimethylsulfoxide/ethanol/dichloromethane solvent mixture after storage for 3 weeks at ambient temperature.

$Tb_2(L)_6(H_2O)_4$ (1). Elemental analysis (%) calcd (found) for $C_{126}H_{116}N_6O_{16}Tb_2$ (2288.15): C, 66.14 (66.38); H, 5.11 (4.75); N, 3.67 (3.89). FT-IR (KBr), ν_{max}: 3429 (ν(O−H)), 1603 (ν_{as}(C═O)), 1572 (ν_{as}(C═O)), 1402 (ν_s(C═O)), 1358 (ν_s(C═O)), 1503, 1221, 1199, 1072, 783 cm^{-1}. MS (FAB) m/z = 1109.06 $(Tb(L)_3) + 1$.

$Eu_2(L)_6(H_2O)_4$ (2). Elemental analysis (%) calcd (found) for $C_{126}H_{116}N_6O_{16}Eu_2$ (2274.23): C, 66.54 (66.82); H, 5.14

(21) Eliseeva, S. V.; Kotova, O. V.; Gumy, F.; Semenov, S. N.; Kessler, V. G.; Lepnev, L. S.; Bünzli, J.-C. G.; Kuzmina, N. P. *J. Phys. Chem. A*. **2008**, *112*, 3614–3626.
(22) Bril, A; De Jager-Veenis, A. W. *J. Electrochem. Soc*. **1976**, *123*, 396–398.
(23) Melhuish, W. H. *J. Opt. Soc. Am*. **1964**, *54*, 183–186.
(24) (a) Mello Donega, C. D.; Junior, S. A.; de Sa, G. F. *Chem. Commun*. **1996**, *11*, 1199–1200. (b) Carlos, L. D.; Mello Donega, C. D.; Albuquerque, R. Q.; Junior, S. A.; Menezes, J. F. S.; Malta, O. L. *Mol. Phys*. **2003**, *101*, 1037–1045.
(25) Sheldrick, G. M. *SHELL-PC*, version 5; Siemens Analytical X-ray Instruments. Inc.: Madison, WI, 1994.

Scheme 1. Synthesis of the Ligand, HL

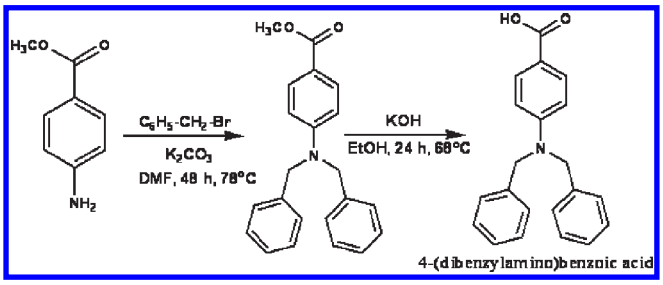

(4.84); N, 3.70 (3.91). FT-IR (KBr), ν_{max}: 3413 (ν(O−H)), 1604 (ν_{as}(C=O)), 1518 (ν_{as}(C=O)), 1403 (ν_s(C=O)), 1358 (ν_s(C=O)), 1495, 1225, 1121, 783 cm^{-1}. MS (FAB) m/z = 1124.7 ($Eu(L)_3$ + Na) + 1.

$Gd_2(L)_6(H_2O)_4$ (3). Elemental analysis (%) calcd (found) for $C_{126}H_{116}N_6O_{16}Gd_2$ (2284.79): C, 66.24 (66.60); H, 5.12 (4.85); N, 3.68 (3.84). FT-IR (KBr), ν_{max}: 3414 (ν(O−H)), 1603 (ν_{as}(C=O)), 1574 (ν_{as}(C=O)), 1395 (ν_s(C=O)), 1356 (ν_s(C=O)), 1513, 1226, 1199, 1078, 946 cm^{-1}. MS (FAB) m/z = 1130.49 ($Gd(L)_3$ + Na) + 1.

Results and Discussion

Synthesis and Characterization of Ligand and Ln^{3+} Complexes 1−3. The ligand 4-(dibenzylamino)benzoic acid (HL) was synthesized in 87% yield according to the method described in Scheme 1. The ligand was characterized by FT-IR, ^{1}H NMR, and ^{13}C NMR spectroscopy (Figure S1 in the Supporting Information) as well as by mass spectroscopy (FAB-MS) and elemental analysis. The synthetic procedures for the Ln^{3+} complexes **1**−**3** are described in the Experimental Section. The microanalyses of complexes **1**−**3** revealed that each Ln^{3+} ion had reacted with the HL ligand in a metal-to-ligand molar ratio of 1:3. The FT-IR spectra of the coordinated ligand HL exhibits two intense bands at approximately 1450 and 1663 cm^{-1}, which are attributable to the symmetric ν_s(C=O) and *anti*-symmetric ν_{as}(C=O) vibration modes, respectively. In each case, coordination of the ligand HL to the respective lanthanide ion was confirmed by the absence of the ν(COOH) absorption bands of the ligand at ∼1660 cm^{-1}. Moreover, the asymmetric and symmetric stretching vibrational modes of the carboxylic acid in complexes **1**−**3** are further split into two peaks [ν_s(C=O): 1402, 1358 cm^{-1}; ν_{as}(C=O): 1603, 1572 cm^{-1} in **1**; ν_s(C=O): 1403, 1358 cm^{-1}; ν_{as}(C=O): 1604, 1518 cm^{-1} in **2**; ν_s(C=O): 1395, 1356 cm^{-1}; ν_{as}(C=O): 1603, 1574 cm^{-1} in **3**]. The difference between the asymmetric and symmetric stretching vibration modes ($\Delta\nu_{(C=O)} = \nu_{as} - \nu_s$) falls in the ranges 245−247 and 170−179 cm^{-1}, which in turn implies that the carboxylate groups are coordinated to the Tb^{3+} or Gd^{3+} ions in two different ways, namely, *via* chelating and bidentate bridging.[26] On the other hand, the difference between the asymmetric and symmetric stretching vibration modes is 246 and 115 cm^{-1} in the case of complex **2**, indicating the coordination of Eu^{3+} with carboxylate groups in chelating and tridentate bridging modes.[26] Furthermore, the IR spectra of **1**−**3** exhibit a broad band at approximately 3400 cm^{-1} which is characteristic of an O−H stretching vibration, thereby indicating the presence of water molecules in the coordination sphere of each complex.

It is clear from the thermogravimetric analysis data for **1** and **2** (Figure S2 in the Supporting Information) that each complex undergoes a mass loss of approximately 3% (calcd, ∼3.14%) in the first step (120−240 °C), which corresponds to elimination of the coordinated water molecules.[27] Subsequent thermal decomposition of **1** and **2** takes place in two steps in the temperature region 240−900 °C. The quantity of residue for each complex represents approximately 16% of the initial mass and corresponds to formation of the respective lanthanide oxide.

X-Ray Crystal Structures. The solid state structures of $Tb_2(L)_6(H_2O)_4$ (**1**) and $Eu_2(L)_6(H_2O)_4$ (**2**) were determined by single-crystal X-ray diffraction. Figures 1 and 2 depict the molecular structures of complexes **1** and **2**, respectively. The pertinent data collection parameters and a listing of significant bond distances and bond angles for the metal coordination environments are presented in Tables 1 and 2, respectively. Compounds **1** and **2** crystallize in the triclinic space group $P\bar{1}$, and their molecular structures consist of homodinuclear species that are bridged by two oxygen atoms from two carboxylate ligands in different coordination modes. It is interesting to note that the dimeric structures of the Ln^{3+}−4-(dibenzylamino)benzoate complexes possess an inversion center of symmetry, thus indicating that the Ln(1) and Ln(2) centers reside in equivalent chemical environments. The distance between the Tb(1) and Tb(2) cations in compound **1** is equal to 4.347 Å, while the corresponding Eu−Eu distance in **2** is 4.309 Å. These distances fall within the range of 3.785−4.532 Å that has been observed for other Ln^{3+} carboxylate complexes that feature both bidentate and tridentate bridging coordination modes.[28] In the case of complex **1**, each terbium atom is coordinated to two η^2-bidentate chelating benzoates, two η^1-carboxylate interactions from the bridging benzoates (the coordination modes can be viewed in Figure 3), which is in good agreement with the IR data. The coordination polyhedra can be described best as distorted square antiprisms, in which six oxygen atoms are furnished by the four benzoate moieties and two oxygen atoms are provided by the two water molecules. The longest Tb−O bonds involve the oxygen atoms of the bidentate chelating ligands [Tb(1)−O(1), 2.458 Å; Tb(1)−O(2), 2.420 Å; Tb(1)−O(4), 2.560 Å; Tb(1)−O(3), 2.358 Å], and the shortest such bonds are associated with the bridging carboxylate ligand [Tb(1)−O(7), 2.330 Å; Tb(1)−O(5), 2.332 Å]. On the other hand, the Tb−O bond distances for the coordinated water molecules [Tb(1)−(O8), 2.421 Å and Tb(1)−O(6), 2.377 Å, respectively] are shorter than those for the bidentate chelating benzoates.[29] Scrutiny of the packing diagram for **1** revealed the presence of a 1D molecular array that is oriented along the *c* axis. This feature is illustrated by the

(26) (a) Deacon, G. B.; Phillips, R. J. *Coord. Chem. Rev.* **1980**, *33*, 227–250. (b) Teotonio, E. E. S.; Brito, H. F.; Felinto, M. C. F. C.; Thompson, L. C.; Young, V. G.; Malta, O. L. *J. Mol. Struct.* **2005**, *751*, 85–94.

(27) Mahata, P.; Ramya, K. V.; Natarajan, S. *Chem.—Eur. J.* **2008**, *14*, 5839–5850.

(28) Cambridge Structural Database, version 5.27. http//www.ccdc.ac.uk (accessed Jan 2010).

(29) Sun, H.-L.; Ye, C.-H.; Wang, X.-Y.; Li, J.-R.; Gao, S.; Yu, K.-B. *J. Mol. Struct.* **2004**, *702*, 77–83.

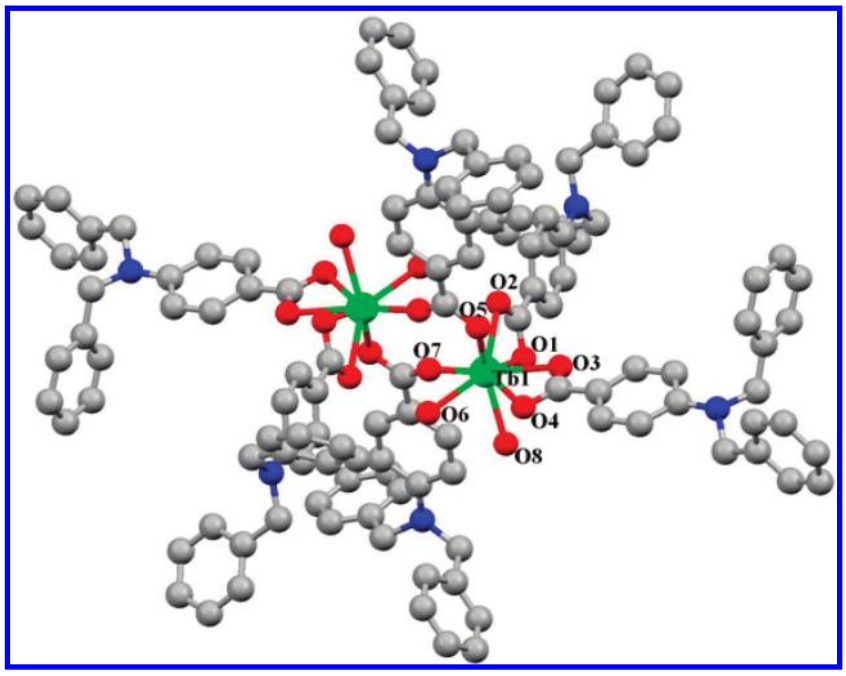

Figure 1. Asymmetric unit of complex **1** with ball and stick model shown at the 30% probability level and all hydrogen atoms omitted for clarity.

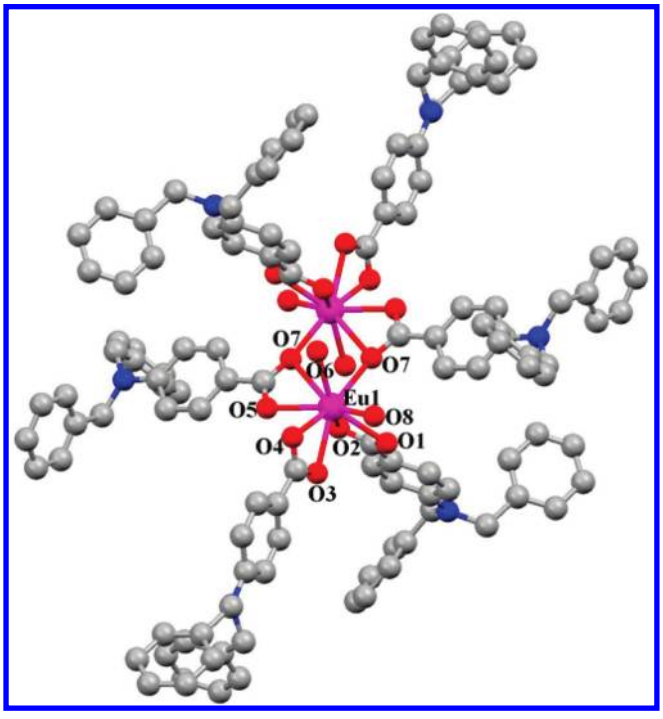

Figure 2. Asymmetric unit of complex **2** with ball and stick model shown at the 30% probability level and all hydrogen atoms omitted for clarity.

intermolecular hydrogen bonding interaction between C28 and O8 through H28 with a H···O distance of 2.650 Å and a C−H···O angle of 154.97° (Figure S3 in the Supporting Information).[30]

In the case of complex **2**, the 4-(dibenzylamino)benzoate ligands exhibit two different coordination modes to the

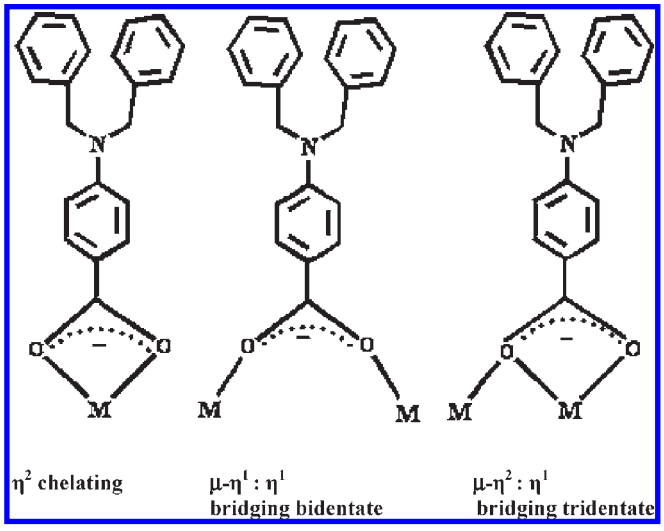

Figure 3. Different types of binding modes for the HL ligand observed in Tb and Eu complexes **1** and **2**.

Table 2. Selected Bond Lengths (Å) and Angles (deg) for **1** and **2**

1		**2**	
Tb1−Tb2	4.347	Eu1−Eu2	4.309
Tb1−O1	2.458(2)	Eu1−O1	2.483(3)
Tb1−O2	2.420(2)	Eu1−O2	2.435(3)
Tb1−O3	2.358(2)	Eu1−O3	2.390(3)
Tb1−O4	2.560(2)	Eu1−O4	2.577(3)
Tb1−O5	2.332(3)	Eu1−O5	2.362(3)
Tb1−O6	2.377(2)	Eu1−O6	2.410(3)
Tb1−O7	2.330(2)	Eu1−O7	2.830(3)
Tb1−O8	2.421(3)	Eu1−O8	2.455(3)
		Eu1−O7#	2.369(3)
O1−Tb1−O2	53.75(8)	O1−Eu1−O2	53.25(10)
O3−Tb1−O4	52.85(7)	O3−Eu1−O4	52.23(10)
O8−Tb1−O6	77.51(8)	O8−Eu1−O6	78.21(10)
O5−Tb1−O7	116.08(9)	O5−Eu1−O7	49.29(9)
O2−Tb1−O5	79.53(8)	O7−Eu1−O7#	68.34(11)
O7−Tb1−O6	74.56(8)	O7−Eu1−O6	75.24(10)
O7−Tb1−O8	92.69(9)	O7−Eu1−O8	92.56(10)

(30) (a) Roesky, H. W.; Andruh, M. *Coord. Chem. Rev.* **2003**, *236*, 91–119. (b) Remya, P. N.; Biju, S.; Reddy, M. L. P.; Cowley, A. H.; Findlater, M. *Inorg. Chem.* **2008**, *47*, 7396–7404.

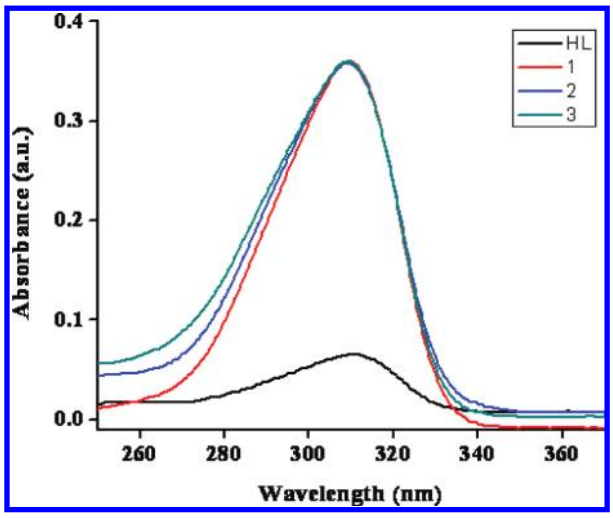

Figure 4. UV−visible absorption spectra of the HL ligand and complexes **1**, **2**, and **3** in $CHCl_3$ solution (2×10^{-6} M).

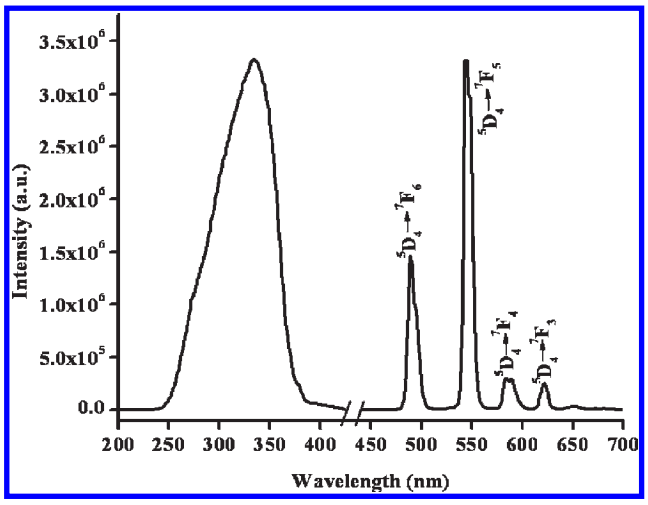

Figure 5. Room-temperature excitation and emission spectra for complex **1** (λ_{ex} = 334 nm) with emission monitored at approximately 545 nm.

Eu^{3+} ions, namely, bidentate chelating (η^2-chelating benzoates) and bidentate chelating with an oxygen atom bridging two metal ions and another oxygen atom coordinating to one of the ions (triply coordinated; η^2-η^1-chelating benzoates), as illustrated in Figure 2, thus corroborating the IR data. The Eu^{3+} ions are nine coordinate and feature two bidentate chelating carboxylates and one tridentate bridging carboxylate ligand. The coordination sphere is completed by the presence of two water molecules. The coordination sphere can be described best as a tricapped trigonal prism in which seven oxygen atoms are provided by four 4-(dibenzylamino)benzoate ligands, and two oxygen atoms are furnished by two water molecules. The Eu−O bond lengths range from 2.362 to 2.830 Å and thus fall within the range anticipated for this type of complex.[11a,15] The longest Eu−O bonds involve the oxygen atoms of one of the triply coordinated ligands [Eu(1)−O(7): 2.830 Å]. Finally, the packing diagram for **2** reveals the presence of a one-dimensional array that is aligned along the *c* axis and which involves an intermolecular hydrogen bonding interaction between the C(28)−H(28) bond of a phenyl ring of one of the carboxylate ligands and the O(8) of a water molecule with a separation of 2.684 Å [H(28)···O(8)] and an angle of 154.44° [C(28)−H(28)−O(8) (Figure S4 in the Supporting Information)].

UV−Vis Spectra. The UV−vis absorption spectrum of the free ligand HL and those of the corresponding complexes **1**−**3** were measured in $CHCl_3$ solution ($c = 2 \times 10^{-6}$ M) and are displayed in Figure 4. The reflectance spectra of complexes **1** and **2** are depicted in Figure S5 (in the Supporting Information). The absorption maxima for **1**−**3** (309 nm), which are attributable to singlet−singlet $^1\pi-\pi^*$ absorptions of the aromatic rings, are slightly blue-shifted with respect to that of the free ligand HL (λ_{max} = 311 nm). No significant changes are apparent in the shapes of the absorption bands upon formation of the lanthanide complexes, therefore suggesting that the coordination of the Ln^{3+} ion does not have a significant influence on the $^1\pi-\pi^*$ transition. However, a small blue shift that is discernible in the absorption maximum of all three complexes is attributable to the perturbation induced by the metal coordination. The molar absorption coefficient values for complexes **1**−**3** at 309 nm of 1.8×10^5, 1.78×10^5, and 1.79×10^5 L mol^{-1} cm^{-1}, respectively, are approximately six times higher than that of the HL ligand (3×10^4 at 311 nm), which is consistent with the presence of six carboxylate ligands in each complex. Note also that the large molar absorption coefficient for the HL ligand indicates that it has a strong ability to absorb light.

Steady-State Photoluminescence. In order to understand the energy transfer processes in the new Ln^{3+} complexes, it was necessary to determine the singlet and triplet energy levels of the ligand, 4-(dibenzylamino)benzoic acid (HL). The singlet ($^1\pi\pi^*$) energy level of this ligand was estimated by reference to the wavelength of the UV−vis absorption edge of the Gd^{3+} complex **3**. The pertinent value was found to be 331 nm (30221 cm^{-1}) in the case of the HL ligand. The triplet energy level ($^3\pi\pi^*$) of this ligand was calculated by reference to the lower wavelength emission edge (423 nm: 23 640 cm^{-1}) from the low-temperature phosphorescence spectra of the Gd^{3+} complex of the 4-(dibenzylamino)benzoic acid (Figure S6 in Supporting Information). According to Reinhoudt's empirical rule, the intersystem crossing process becomes effective when ΔE ($^1\pi\pi^* - {}^3\pi\pi^*$) is at least 5000 cm^{-1}.[31] The energy gap ΔE ($^1\pi\pi^* - {}^3\pi\pi^*$) for the ligand HL is 6581 cm^{-1}; hence, our new complexes amply satisfy this condition. As a consequence, the intersystem crossing process is effective for this ligand. The triplet energy level of HL appears at appreciably higher energy than $^5D_4$ for Tb^{3+} or $^5D_0$ for Eu^{3+}, thus indicating that the designed new ligand can act as an antenna for the photosensitization of trivalent Ln^{3+} ions.

The solid-state excitation and emission spectra of complex **1** recorded at room temperature are displayed in Figure 5. The excitation spectrum monitored at the characteristic emission of the Tb^{3+} ion in the solid state overlaps with the absorption spectrum in the 250−360 nm region (Figure 4), which indicates that energy transfer from the ligand to the metal ion is operative. The excitation spectrum of **1** exhibits a broad band between 250 and 380 nm which is attributable to the $\pi-\pi^*$ transition of the

(31) Steemers, F. J.; Verboom, W.; Reinhoudt, D. N.; Vander Tol, E. B.; Verhoeven, J. W. *J. Am. Chem. Soc.* **1995**, *117*, 9408–9414.

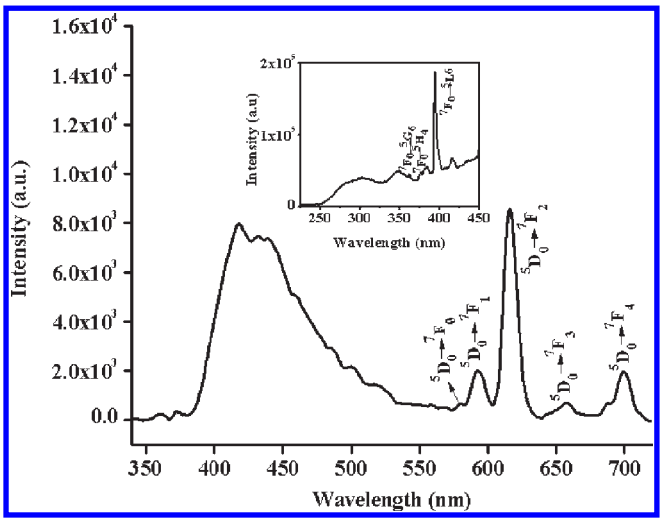

Figure 6. Room-temperature excitation (inset) and emission spectra for complex **2** (λ_{ex} = 308 nm) with emission monitored at approximately 612 nm.

aromatic carboxylate ligand. The absence of any absorption bands due to the f−f transitions of the Tb^{3+} cation proves that luminescence sensitization *via* excitation of the ligand is effective. The room-temperature emission spectrum of complex **1** exhibits the characteristic emission bands of the Tb^{3+} cation (λ_{ex} = 334 nm) centered at 488, 545, 585, and 620 nm which result from deactivation of the $^5D_4$ excited state to the corresponding ^7F_J ground state of the Tb^{3+} cation (J = 6, 5, 4, 3).[11,30b,32] Interestingly, no emission bands from the organic ligand were observed, which leads to the conclusion that energy transfer from the ligand to the Tb^{3+} center is very efficient.

The solid-state excitation and emission spectra for the Eu^{3+} complex **2** at room temperature are shown in Figure 6. The excitation spectrum of the Eu^{3+} complex of HL has negligible contributions from the ligand and exhibits a series of sharp lines that are characteristic of the Eu^{3+} energy-level structure and can therefore be assigned to transitions between the $^7F_{0,1}$ and $^5L_6$ and $^5D_{2,1}$ levels.[9c,31,33] Accordingly, luminescence sensitization of the Eu^{3+} complex *via* ligand excitation is not efficient in this case. The ambient-temperature emission spectrum of the Eu^{3+} complex is characteristic of the metal in the 550−700 nm region and exhibits well-resolved peaks that are attributable to transitions from the metal-centered $^5D_0$ excited state to the ^7F_J ground-state multiplet. Maximum peak intensities at 580, 593, 617, 652, and 694 nm were observed for the J = 0, 1, 2, 3, and 4 transitions, respectively, and the J = 2 so-called "hypersensitive" transition is intense.[9c,33,34] The intensity of the $^5D_0 \rightarrow {}^7F_2$ transition (electric dipole) is greater than that of the $^5D_0 \rightarrow {}^7F_1$ transition (magnetic dipole), which indicates that the coordination environment of the Eu^{3+} ion is devoid of an inversion center. Furthermore, an intense broad band in the region 400−500 nm due to a $\pi-\pi^*$ transition of the ligand was evident in the emission spectrum of **2**. Such an observation is typically diagnostic of poor sensitization of the ligand toward the Eu^{3+} ion.

The luminescent lifetimes of Ln^{3+} complexes **1** and **2** were measured at both ambient (298 K) and low temperatures (77 K) on the basis of the respective luminescent decay profiles by fitting them with monoexponential decay curves (Figures S7 and S8 in the Supporting Information). Collectively, these data imply the existence of a single chemical environment around the Ln^{3+} ion in each case. The pertinent values are summarized in Table 3. A longer $^5D_4$ lifetime value (τ_{obs} = 1.02 ms) was observed in the case of the Tb^{3+} complex **1** despite the presence of solvent molecules in the first coordination sphere, since such molecules are typically vibrational deactivators of the excited states of Ln^{3+} ions. It is somewhat surprising that the magnitude of the $^5D_4$ lifetime for complex **1** is not very high compared with some recently reported data for highly luminescent Tb^{3+} complexes ($\Phi_{overall}$ = 56%; τ_{obs} = 2.63 ms).[35] On the other hand, there is a recent report of a $\Phi_{overall}$ value of 40% and τ_{obs} = 0.46 ms for Tb^{3+}−dipivaloylmethanato complexes.[21] Furthermore, the present authors also observed a $\Phi_{overall}$ value of 72% and τ_{obs} = 0.92 ms for a Tb^{3+}−4-isobutyryl-3-phenyl-5-isoxazolonate complex.[32a] The lifetime is the inverse of the total deactivation rate, which in turn is the sum of the radiative and nonradiative rates. Therefore, the fact that a lanthanide complex is highly luminescent yet possesses a short lifetime does not represent a contradiction. It simply means that the radiative rate is rapid, as observed in the case of Tb^{3+} complex **1**. Moreover, on account of its electronic structure, the Tb^{3+} cation has many energy levels that can mix with appropriate ligand wave functions, including a relatively low-lying 4f5d state, which may explain why the lifetime is relatively short (i.e., it implies that the phosphorescence character of the transition is partly lost). The somewhat shorter $^5D_0$ lifetime value (τ_{obs} = 0.33 ms) that was observed for the Eu^{3+} analogue may be due to the dominant nonradiative decay channels associated with vibronic coupling due to the presence of solvent molecules. Similar observations have been made for several europium complexes.[9c,36]

In order to gain a better understanding of the luminescence efficiencies of the new 4-(dibenzylamino)benzoate complexes **1** and **2**, it was appropriate to calculate the overall quantum yields. The overall quantum yield

(32) (a) Biju, S.; Reddy, M. L. P.; Cowley, A. H.; Vasudevan, K. V. *J. Mater. Chem.* **2009**, *19*, 5179–5187. (b) Xia, J.; Zhao, B.; Wang, H.-S.; Shi, W.; Ma, Y.; Song, H.-B.; Cheng, P.; Liao, D.-Z.; Yan, S.-P. *Inorg. Chem.* **2007**, *46*, 3450–3458. (c) Carnall, W. T. In *Handbook on the Physics and Chemistry of Rare Earths*; Gschneidner, K. A., Eyring, L., Eds.; Elsevier: Amsterdam, The Netherlands, 1987; Vol. *3*, Chapter 24, pp 171−208. (d) Dieke, G. H. *Spectra and Energy levels of Rare Earth Ions in Crystals*; Interscience: New York, 1968.

(33) (a) Pavithran, R.; Reddy, M. L. P.; Junior, S. A.; Freire, R. O.; Rocha, G. B.; Lima, P. P. *Eur. J. Inorg. Chem.* **2005**, *20*, 4129–4137. (b) Zucchi, G.; Olivier, M.; Pierre, T.; Gumy, F.; Bünzli, J.-C. G.; Michel, E. *Chem.—Eur. J.* **2009**, *15*, 9686–9696. (c) Kajiwara, T.; Hasegawa, M.; Ishii, A.; Katagiri, K.; Baatar, M.; Takaishi, S.; Iki, N.; Yamashita, M. *Eur. J. Inorg. Chem.* **2008**, *36*, 5565–5568.

(34) (a) Ambili Raj, D. B.; Biju, S.; Reddy, M. L. P. *Dalton Trans.* **2009**, *36*, 7519–7528. (b) Fu, L.; Sa Ferreira, R. A.; Silva, N. J. O.; Fernandes, A. J.; Ribeiro-Carlo, P.; Gonalves, I. S.; de Zea Bermudez, V.; Carlos, L. D. *J. Mater. Chem.* **2005**, *15*, 3117–3125. (c) Pavithran, R.; Saleesh Kumar, N. S.; Biju, S.; Reddy, M. L. P.; Alves, S., Jr.; Freire, R. O. *Inorg. Chem.* **2006**, *45*, 2184–2192. (d) Werts, M. H. V.; Jukes, R. T. F.; Verhoeven, J. W. *Phys. Chem. Chem. Phys.* **2002**, *4*, 1542–1548.

(35) Samuel, A. P. S.; Moore, E. G.; Melchior, M.; Xu, J.; Raymond, K. N. *Inorg. Chem.* **2008**, *47*, 7535–7544.

(36) Ambili Raj, D. B.; Biju, S.; Reddy, M. L. P. *Inorg. Chem.* **2008**, *47*, 8091–8100.

Table 3. Radiative (A_{RAD}) and Nonradiative (A_{NR}) Decay Rates, $^5D_0/^5D_4$ Lifetimes (τ_{obs}), Radiative Lifetimes (τ_{RAD}), Intrinsic Quantum Yields (Φ_{Ln}), Energy Transfer Efficiencies (Φ_{sen}), and Overall Quantum Yields ($\Phi_{overall}$) for Complexes **1** and **2**

complex	A_{RAD}/s^{-1}	A_{NR}/s^{-1}	$\tau_{obs}/\mu s$	$\tau_{RAD}/\mu s$	Φ_{Ln} (%)	Φ_{sen}(%)	$\Phi_{overall}$ (%)
1			1020 ± 0.8	1040 ± 0.8	98	84	82 ± 8^a
						87	85 ± 8^b
2	212	2812	330 ± 1	4720 ± 1	7.0	0.14	$< 0.01^a$

[a] Absolute quantum yield. [b] Relative quantum yield.

($\Phi_{overall}$) for a lanthanide complex treats the system as a "black box" in which the internal process is not considered explicitly. Given that the complex absorbs a photon (i.e., the antenna is excited), the overall quantum yield can be defined as follows:[37]

$$\Phi_{overall} = \Phi_{sen}\Phi_{ln} \quad (2)$$

Here, Φ_{sen} represents the efficiency of the energy transfer from the ligand to the Ln^{3+} ion and Φ_{Ln} represents the intrinsic quantum yield of the Ln^{3+} ion, which can be calculated from the following equation:

$$\phi_{ln} = \left(\frac{A_{RAD}}{A_{RAD} + A_{NR}}\right) = \frac{\tau_{obs}}{\tau_{RAD}} \quad (3)$$

In the case of the Eu^{3+} complex **2**, the radiative lifetime (τ_{RAD}) can be calculated using eq 4,[15,7d] assuming that the energy of the $^5D_0 \rightarrow {}^7F_1$ transition (MD) and its oscillator strength are constant.

$$A_{RAD} = \frac{1}{\tau_{RAD}} = A_{MD,0}n^3\left(\frac{I_{TOT}}{I_{MD}}\right) \quad (4)$$

Hence, $A_{MD,0}$ (14.65 s^{-1}) represents the spontaneous emission probability of the $^5D_0 \rightarrow {}^7F_1$ transition in vacuo, I_{TOT}/I_{MD} is the ratio of the total area of the corrected Eu^{3+} emission spectrum to the area of the $^5D_0 \rightarrow {}^7F_1$ band, and n is the refractive index of the medium. An average index of refraction equal to 1.5 was employed in the calculation.[34c] The intrinsic quantum yield for Tb^{3+} (Φ_{Tb}) was estimated by means of eq 5 with the assumption that the decay process at 77 K in a deuterated solvent is purely radiative.[18,32a,38]

$$\phi_{Tb} = \frac{\tau_{obs(298\ K)}}{\tau_{RAD(77\ K)}} \quad (5)$$

The overall quantum yields ($\Phi_{overall}$), radiative (A_{RAD}) and nonradiative (A_{NR}) decay rates, intrinsic quantum yields (Φ_{Ln}), and energy transfer efficiencies (Φ_{sen}) for complexes **1** and **2** are presented in Table 3. In the solid state, the overall quantum yields for these complexes were determined according to the absolute method of Wrighton et al.[39,19a] A remarkably high quantum yield value of 82% has been observed for the Tb−4-(dibenzylamino)benzoate complex **1**. This large value is particularly surprising in view of the presence of four H_2O molecules in the first coordination sphere, since such solvent molecules typically serve as vibrational deactivators of the excited states of Ln^{3+} ions. Only a few Tb^{3+} complexes have been reported to exhibit higher quantum yields in the solid state.[17,33b,33c] Recently, the present authors reported another case of a high quantum yield (72%) for a 4-isobutyryl-3-phenyl-5-isoxazolonate complex of Tb^{3+} that also features solvent molecules in the primary coordination sphere.[32a] The energy gap between the luminescent state and the ground state manifold is approximately 12 000 cm^{-1} for Eu^{3+} and 14 800 cm^{-1} for Tb^{3+}. Relatively efficient coupling of the Eu^{3+} excited states occurs to the third vibrational overtone of proximate OH oscillators ($\nu_{OH} \sim 3300-3500$ cm^{-1}), and to the fourth harmonic in the case of Tb^{3+}, which is consistent with the observation of less efficient quenching for Tb^{3+}, when the Franck−Condon overlap factor is less favorable.[40]

It is well recognized that the energy-level match between the triplet states of the ligands to the ^5D_J state of the Ln^{3+} cation is one of the key factors that governs the luminescence efficiency of Ln^{3+} complexes.[41] Latva's empirical rule states that an optimal ligand-to-metal energy transfer process for Ln^{3+} requires ΔE ($^3\pi\pi^* - {}^5D_4$) = 2500−4500 cm^{-1} for Tb^{3+} and 2500−4000 cm^{-1} for Eu^{3+}.[42] On this basis, it can be concluded that the energy transfer to the Tb^{3+} ion will be more effective for the ligand 4-(dibenzylamino)benzoic acid, since ΔE ($^3\pi\pi^* - {}^5D_4$) for **1** is 3140 cm^{-1}. The very high intrinsic quantum yield (Φ_{Ln}) and energy transfer efficiency (Φ_{sen}) for complex **1** further confirms the view that 4-(dibenzylamino)benzoic acid is an efficient sensitizer for the Tb^{3+} ion. Poor luminescence efficiency ($\Phi_{overall} < 0.01$) is also apparent in complex **2** and may be due to the weak sensitization efficiency ($\Phi_{sen} = 0.14\%$) of 4-(dibenzylamino)benzoic acid with respect to the Eu^{3+} ion. The latter observation can be explained on the basis of the large energy gap between the triplet state of the ligand (6340 cm^{-1}) and the $^5D_0$ emitting level of the Eu^{3+} ion (17 300 cm^{-1}).

Conclusions

A novel efficient antenna complex of Tb^{3+} supported by the 4-(dibenzylamino)benzoic acid ligand has been designed,

(37) (a) Xiao, M.; Selvin, P. R. *J. Am. Chem. Soc.* **2001**, *123*, 7067–7073. (b) Quici, S.; Cavazzini, M.; Marzanni, G.; Accorsi, G.; Armaroli, N.; Ventura, B.; Barigelletti, F. *Inorg. Chem.* **2005**, *44*, 529–537. (c) Comby, S.; Imbert, D.; Anne-Sophie, C.; Bünzli, J.-C. G.; Charbonniere, L. J.; Ziessel, R. F. *Inorg. Chem.* **2004**, *43*, 7369–7379.

(38) Nasso, I.; Bedel, S.; Galaup, C.; Picard, C. *Eur. J. Inorg. Chem.* **2008**, *12*, 2064–2074.

(39) Wrighton, M. S.; Ginley, D. S.; Morse, D. L. *J. Phys. Chem.* **1974**, *78*, 2229–2233.

(40) (a) Dossing, A. *Eur. J. Inorg. Chem.* **2005**, *8*, 1425–1434. (b) Beeby, A.; Clarkson, I. M.; Dickins, R. S.; Faulkner, S.; Parker, D.; Royle, L.; de Sousa, A. S.; Williams, J. A. G.; Woods, M. *J. Chem. Soc., Perkin Trans. 2* **1999**, *3*, 493–503.

(41) (a) Shi, M.; Li, F.; Yi, T.; Zhang, D.; Hu, H.; Huang, C. *Inorg. Chem.* **2005**, *44*, 8929–8936. (b) Xin, H.; Shi, M.; Gao, X. C.; Huang, Y. Y.; Gong, Z. L.; Nie, D. B.; Cao, H.; Bian, Z. Q.; Li, F.; Huang, C. H. *J. Phys. Chem. B.* **2004**, *108*, 10796–10800.

(42) Latva, M.; Takalo, H.; Mukkala, V. M.; Matachescu, C.; Rodriguez-Ubis, J. C.; Kanakare, J. *J. Lumin.* **1997**, *75*, 149–169.

synthesized, and characterized and its photophysical properties evaluated. The new aromatic carboxylate complex of Tb^{3+} exhibits bright green luminescence efficiency in the solid state with a quantum yield of 82%, thus rendering it an excellent candidate for use in various photonic applications. The high quantum yield is attributable to the superior match of the triplet energy level of the ligand with that of the $^5D_4$ emitting level of Tb^{3+}. By contrast, the poor sensitization observed for the corresponding Eu^{3+} complex is mainly due to the larger energy gap between the ligand triplet state and $^5D_0$ level of Eu^{3+}.

Acknowledgment. The authors acknowledge financial support from the Department of Science and Technology (SR/S1/IC- 36/2007) and the Council of Scientific and Industrial Research, New Delhi (NWP0010). A.R.R. thanks CSIR, New Delhi for the award of Junior Research Fellowship. A.H.C. thanks the Robert A. Welch Foundation (F-0003) for financial support.

Supporting Information Available: X-ray crystallographic data of complexes **1** and **2** in CIF format, ^1H and ^{13}C NMR spectra for ligand HL, thermogravimetric data, view of complexes **1** and **2** showing the intermolecular hydrogen bonding interactions, reflectance spectra of complexes **1** and **2**, phosphorescence spectrum of gadolinium complex **3** at 77 K, and luminescence decay profiles. This material is available free of charge via the Internet at http://pubs.acs.org.